**SYLWESTER KANIA[1,2], JANUSZ KULIŃSKI[2],
DOMINIK SIKORSKI[3]**

[1]Institute of Physics, Lodz University of Technology, ul. Wólczańska 219,
90-924 Łódź, Poland, e-mail: sylwester.kania@p.lodz.pl
[2]Centre of Mathematics and Physics, Lodz University of Technology,
Al. Politechniki 11, 90-924 Łódź, Poland, e-mail: janusz.kulinski@p.lodz.pl
[3]Faculty of Material Technologies and Textile Design, Department of material
and commodity sciences and textile metrology, Lodz University of Technology,
ul. Żeromskiego 116, 90-924 Łódź, Poland, e-mail: dominik.junior@wp.pl

ELECTRICAL AND THERMAL PROPERTIES
OF ANTHRONE

Quantum-chemical density functional theorem (DFT) calculations indicate that the value of the reorganization energy indicates the possibility of efficient hole capture by the anthrone molecule during transport process of charge carriers. Differential scanning calorimetry (DSC) studies indicate the temperature stability of anthrone molecules above the melting point up to 164°C. The glass transition is determined at 153.7 °C and melting point at 157.05 °C.

Keywords: anthrone, differential scanning calorimetry (DSC), reorganization energy, DFT calculations.

1. INTRODUCTION

Understanding the microscopic processes determining the charge carrier mobility in organic materials is essential for improvement of the quality of existing devices made of organic semicnductors [1,2]. In this article we continue our studies on different aspects of anthrone and anthraquinone as the derivatives of anthracene [3,4,5]. We describe the results of our investigation on the development of DFT calculations and DSC measurements.

The structure of anthrone ($C_{14}H_{10}O$), is monoclinic with space group $C_{2h5}(P_{21/a})$ with bimolecular unit of the dimensions (in room temperature) $a_0 = (15.80\pm0.03)$ Å, $b_0 = (3.998\pm0.005)$ Å, $c_0 = (7.86\pm0.16)$ Å, $\beta = 101°40'$ [6,7]. The non-centrosymmetric anthrone molecules of anthrone are

characterised with large dipole moment of 3.5 D ($1.19 \cdot 10^{-29}$ Cm) (in benzene) [8]. X-ray determination of the structure of anthrone is hindered by the fact that orientation of the molecules in the unit cell is arranged statistically (determined by the direction and sense of dipole moment vector strictly correlated with the position of the oxygen atom) [6,7]. Therefore, solid anthrone possesses higher symmetry than would be expected for two asymmetric molecules present in the unit cell. The bond dimensions in the molecule of anthrone are shown in Fig. 1.
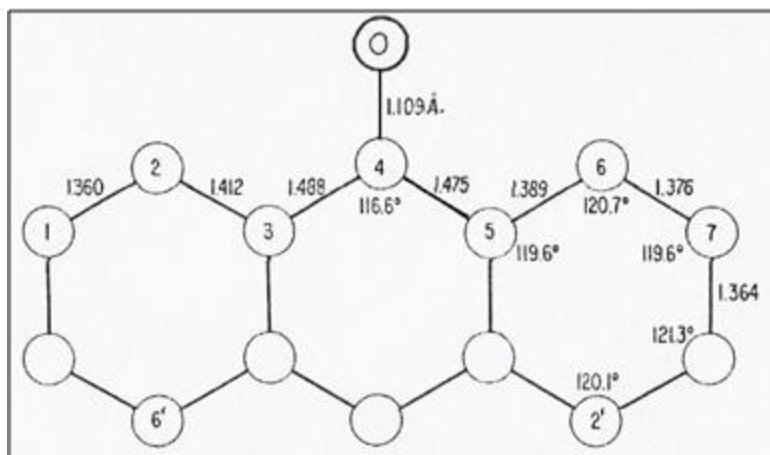

Fig. 1. Bonds' dimensions in the molecule of anthrone

1. DFT CALCULATIONS

The quantum-chemical calculations were carried out with use of density functional theorem (DFT) with GAUSSIAN09 program [9]. The structures of anthraquinone and anthrone were optimized at B3LYP (Becke three parameter (exchange), Lee Yang, and Parr [10]) method using 6-311+g(d,p) basis set.. The energy of high occupied molecular orbital (HOMO), and energy of low unoccupied molecular orbital (LUMO) and band gap calculations, based on the optimized geometric structure, were performed with the same level of theorem at the ground, cation and anion states. The calculations were made for the molecules being in the gas state [11].

The "four-point" [12,13] method (equations (1) and (2)) was used to calculate the reorganization energy λ. The theoretical description of the conductivity of the molecular system is characterized by weak electronic coupling. Therefore, one needs to take into account the fact that nuclear

dynamics is much slower than the dynamics of charge carriers. Thus, we can divide the whole system into two subsystems, the fast one related to the electron cloud and the slow one related to the nuclei of the atoms that make up the molecule.

When the neutral organic molecule is charged during hole transport, it forms cationic open-shell electronic configuration which corresponds to process of oxidation [14]

$$M \rightarrow M^+ + e^-. \tag{1}$$

The energy change connected with this charge transfer is called the internal reorganization energy (λ^{int}). Electronic polarization of surrounding molecules is connected with external reorganization energy (λ^{ext}).

The total reorganization energy of the molecule may be described as a sum of internal and external terms:

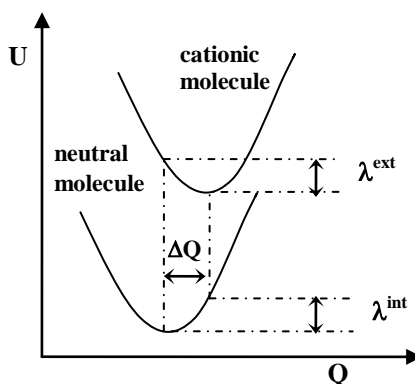$$\lambda_{ij} = \lambda^{int} + \lambda^{ext} \tag{2}$$

Fig. 2. Schematic representation of the potential energy surfaces of the neutral and cationic molecules. (Q-reaction coordinate, U- potential energy)

In the high temperature limit, the transfer rate for a charge to hop from a site *i* to a final site *j* is [14, 15]:

$$k_{ij} = \frac{2\pi}{\hbar} \frac{J_{ij}^2}{\sqrt{4\pi\lambda_{ij}k_BT}} \exp\left[-\frac{(\Delta E_{ij} - \lambda_{ij})^2}{4\lambda_{i\alpha}k_BT} \right], \tag{3}$$

where T is temperature, k_B is Boltzmann constant, ΔE_{ij} is the difference of electron energy between the initial and final molecular sites, $\hbar$ is the reduced Planck constant, J_{ij} is a transfer integral describing electron transfer between i and j molecule.

The results of calculations are presented in the Table 1. We observe the difference between values obtained from the ground energy of the molecules and the energy calculated by Koopmans' theorem [15] which does not take into account the correlation effect of the nuclei in the atoms in molecule .

Table 1

Calculated with DFT B3LYP 6/3111++G(d,p) reorganization energy λ, charge transfer integral J and rate of charge transfer k_e for anthrone

		Four point method - total ground energy of the molecule	Four point method - Koopmans' theorem
λ, holes	[eV]	0.17	0.21
λ, electrons	[eV]	0.37	0.02
J, holes	[eV]	0.024	0.024
J, electrons	[eV]	0.43	0.43
k_e, holes	[Hz]	$4.6 \cdot 10^{12}$	$2.9 \cdot 10^{14}$
k_e, electrons	[Hz]	$1.4 \cdot 10^{14}$	$1.7 \cdot 10^{16}$

2. DSC MEASUREMENTS

The measurement method of differential scanning calorimetry (DSC) allows to determine the stability of the compound at melting temperature. The DSC method measures the temperatures and heat flows associated with transitions in materials in controlled atmosphere as a function of time and temperature. The differences in the amount of heat required to increase the temperature of a sample and reference are recorded as a function of time and temperature. The DSC measurement allows qualitative and quantitative determination of physical and chemical changes associated with endothermic and exothermic processes, as well as changes in heat capacity.

The measurements were made using a TA Instruments Universal Analysis Q2000 computer-controlled research-grade DSC device for temperature and heat flow regulation. The TA Instruments Universal Analysis program for Windows was used as a data analysis program. The program allows to select the type and region to be analysed, the type of transition analysis, and determine which transition should be analysed. Cell schematic diagram is presented in Fig. 3.
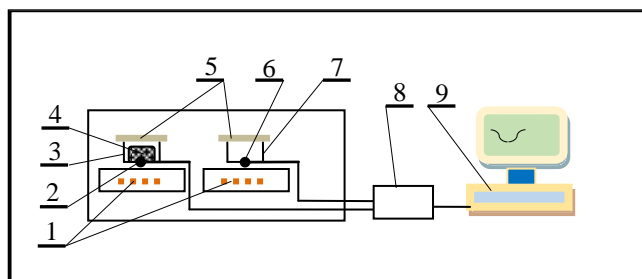
Fig. 3. Cell schematic diagram of DSC apparatus, 1 – heaters, 2 – measuring thermocouple junction, 3 – sample pan, 4 – sample, 5 – covers, 6 – reference thermocouple junction, 7 – reference sample pan, 8 – interface, 9 – computer reading the temperature and regulating heat flow

The DSC technique allows to minimize the number of samples to perform the analysis due to the automation of its precision measurement. Thermal analysis is performed automatically on small samples. The measurements were made with anthrone with purity grade > 99 % (HPLC) from Fluka with flash point (150±17)°C and melting point in the range of 153-160°C and boiling point 721°C. Density of anthrone was 1.0550 g/cm^3.
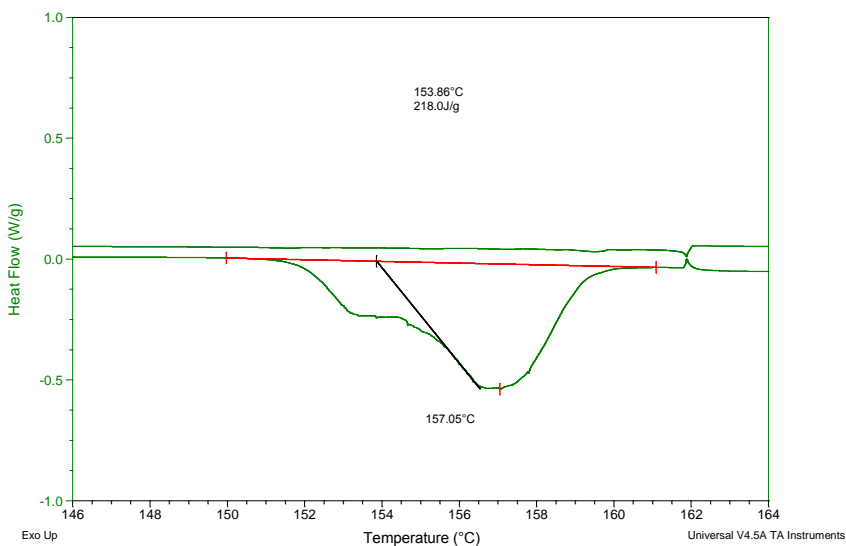

Fig. 4. Determination of anthrone melting point by DSC method, thermogram for the entire measuring range

DSC curve is presented in Fig. 4. The sample mass was 12.060 mg and the measurements were made in the ambient of nitrogen gas. Heating rate was 0.35°C/min, start temperature was 146°C and final temperature 164°C.

Melting temperature of anthrone was determined to be $T_c = 157.05°C$ (Fig. 2). The examined material did not decompose after passing through the melting point. The glass transition temperature (Fig 3) is observed between first deviation temperature $T_0 = 151.2°C$ and comeback to baseline temperature $T_r = 154.2°C$. The midpoint temperature $T_g = 153.7°C$ was determined as average of the extrapolated threshold temperature T_f and extrapolated final temperature T_e. The midpoint temperature was taken as the glass transition temperature.
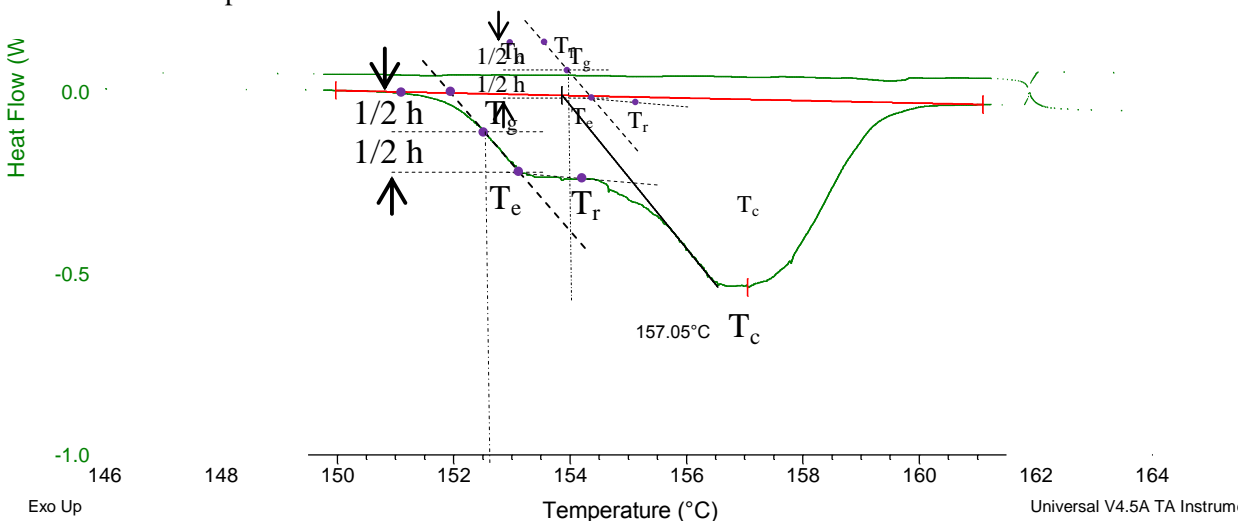

Fig. 5. Determination of anthrone glass transition temperature T_g. (Parameters influencing determination of T_g: $T_0 = 151.2°C$ first deviation temperature, $T_f = 152.1°C$ – extrapolated threshold temperature, $T_g = 153.7°C$ – midpoint temperature, $T_e = 153.3°C$ – extrapolated final temperature, $T_r = 154.2°C$ – comeback to baseline temperature). Heating rate 0.35°C/min. Type of transition – sigmoidal.

4. DISCUSSION AND CONCLUSIONS

The obtained melting temperature of anthrone $T_c = 157.05°C$ (see Fig. 5) cannot be determined precisely what is associated with the appearance of amorphous and polycrystalline phase during transition into melt taking place in the range of 156.6°C - 157.1°C. During melting, anthrone molecule does not

decompose. The glass transition temperature for anthrone appears about 153°C, *i.e.* above the operating temperatures of electronic devices used in commercial applications at room temperatures. That is why anthrone is interesting from the point of view of organic electronics applications.

During transport of charge carriers through the material, the charge transfer through the molecules must occur. This charge transfer through molecule can be interpreted as an occurrence of red-ox processes [14].

The DFT calculations show that for the hole conductivity, the reorganization energy obtained by the "four-point" method using ground states and using Koopmans' theorem are similar. The difference between reorganization energies is about 15%. This difference is related to taking into account the correlation energy in the calculations carried out in the "four-point" method with the use of ground states compare with ones based on Koopmans' theorem. This result proves that these reactions can be reversible without permanent ionizing the molecule while the charge is transported through the layer.

On the contrary, when the reorganization energy for electronic conductivity is calculated, a significant difference between the values obtained from the ground states and the Koopmans' theorem is observed. This may be due to the fact that the gas phase anionic anthrone particle does not have bonding electronic states at the LUMO energy level [5]. It also leads to a significant overestimation of the value of electron transfer rate by two orders of magnitude in the Koopmans' method calculations.

The glass transition above 100°C (T_g = 153.7°C) allows the anthrone to be used for applications in the home electronics. The anthrone molecule does not dissociate which makes this compound a promising material for applications in organic electronics

5. ACKNOWLEDGEMENTS

REFERENCES

[1] Minder N., A., Ono S., Chen Z., Facchetti A., Morpurgo A. 2012. Band-like electron transport in organic transistors and implication of the molecular structure for performance optimization. Adv. Mater. 24: 503–508. DOI: 10.1002/adma. 201103960

[2] Kwon J., Takeda Y., Shiwaku R., Tokito S., Cho K., Jung S. 2019. Three-dimensional monolithic integration in flexible printed organic transistors. Nat. Commun., 10: 54-1-54-9. https://doi.org/10.1038/s41467-018-07904-5

[3] Kania S., Kościelniak-Mucha B., Kuliński J., Słoma P. 2015. Effect of molecule dipole moment on hole conductivity of polycrystalline anthrone and anthrachinone layers. Sci. Bull. Techn. Univ. Lodz, Physics, 36: 13-25. http://cybra.lodz.pl/dlibra/publication/17133/edition/13805/content

[4] Kania S., Kuliński J., Sikorski D. 2019. Electrical and thermal properties of anthraquinone layers. Sci. Bull. Techn. Univ. Lodz, Physics, 40: 13-25. https://doi.org/10.34658/physics.2019.40.13-25

[5] Kania S., Kościelniak-Mucha B., Kuliński J., Słoma P., Wojciechowski K. 2019. Polarization of organic aromatic molecule in anionic and cationic state. Sci. Bull. Techn. Univ. Lodz, Physics, 40: 27-35. https://doi.org/10.34658/physics.2019.40.27-35

[6] Harris J.W. 1965. Mixed anthrone-antraquinone crystals. Nature 206:1038. https://doi.org/ 10.1038/2061038a0

[7] Srivastava S.N. 1962. Crystal structure of anthrone. Z. Krist. 117: 5-6, 386-398. DOI: 10.1524/zkri.1962.117.5-6.386

[8] Angyal C.L., Le Fevre R.J.W. 1950. The polarities of enols. J. Chem. Soc., 106: 562-564. https://doi.org/10.1039/JR9500000562

[9] Gaussian 09, Revision A.02. 2009. Frisch M.J., Trucks G.W., Schlegel H.B., Scuseria G.E., Robb M.A., Cheeseman J.R., Scalmani G., Barone V., Mennucci B., Petersson G.A., Nakatsuji H., Caricato M., Li X., Hratchian H.P., Izmaylov A.F., Bloino J., Zheng G., Sonnenberg J.L., Hada M., Ehara M., Toyota K., Fukuda R., Hasegawa J., Ishida M., Nakajima T., Honda Y., Kitao O., Nakai H., Vreven T., Montgomery J.A., Peralta Jr. J.E., Ogliaro F., Bearpark M., Heyd J.J., Brothers E., Kudin K.N., Staroverov V.N., Kobayashi R., Normand J., Raghavachari K., Rendell A., Burant J.C., Iyengar S.S., Tomasi J., Cossi M., Rega N., Millam J.M., Klene M., Knox J.E., Cross J.B., Bakken V., Adamo C., Jaramillo J., Gomperts R., Stratmann R.E., Yazyev O., Austin A.J., Cammi R., Pomelli C., Ochterski J.W., Martin R.L., Morokuma K., Zakrzewski V.G., Voth G.A., Salvador P., Dannenberg J.J., Dapprich S., Daniels A.D., Farkas O., Foresman J.B., Ortiz J.V., Cioslowski J., Fox D.J., Wallingford C.T.: Gaussian, Inc.

[10] Becke A.D. 1993. Density-functional thermochemistry. III. The role of exact exchange. J. Chem. Phys. 98: 5648-5652. https://doi.org/10.1063/1.464913

[11] Skobel'tsyn D.V. 1966. Chapter III. The oriented gas model and its application to molecular crystals polarization diagrams of luminescence. in: Physical optics. The Lebedev Physics Institute series. 25: 44-66. DOI: 10.1007/978-1-4684-7206-6_3

[12] Datta A., Mohakud S., Pati S.K. 2007. Electron and hole mobilities in polymorphs of benzene and naphthalene: role of intermolecular interactions. J. Chem. Phys. 126: 144710-1-144710-6. https://doi.org/10.1063/1.2721530

[13] Rühle V., Lukyanov A., Falk M., Schrader M., Vehoff T., Kirkpatrick J., Baumeier B., Andrienko D. 2010.Microscopic simulations of charge transport in disordered organic semiconductors. J. Chem. Theor. Comput. 7: 3335-3345.

[14] Marcus R.A. 2000. Tutorial on rate constants and reorganization energies. J. Electroanalytical Chem. 483: 2-6. https://doi.org/10.1016/S00220728(00)00011-5

[15] Tsuneda T., Song J.-W., Suzuki S., Hirao K. 2010. On Koopmans' theorem in density functional theory. J. Chem. Phys. 133: 174101-1-174101-9. https://doi.org/10.1063/1.3491272

ELEKTRYCZNE I TERMICZNE WŁASNOŚCI ANTRONU

Streszczenie

Obliczenia funkcjonału kwantowo-chemicznego (DFT) wskazują, że wartość energii reorganizacji wskazuje na możliwość efektywnego wychwytywania dziur przez cząsteczkę antronu podczas transportu nośników ładunku. Badania metodą różnicowej kalorymetrii skaningowej (DSC) wskazują na stabilność temperaturową cząsteczek antronu powyżej temperatury topnienia do 164°C. Temperaturę zeszklenia określono jako $T_g = 153{,}7°C$, a temperaturę topnienia jako $T_c = 157{,}05°C$.